Methods for Estimating Hydrogen Fuel Tank Characteristics

Nicholas A. Klymyshyn[1]
Mem. ASME
Pacific Northwest National Laboratory,
902 Battelle Boulevard,
P.O. Box 999,
MSIN K9-89,
Richland, WA 99352
e-mail: nicholas.klymyshyn@pnnl.gov

Kriston Brooks
Pacific Northwest National Laboratory,
902 Battelle Boulevard,
P.O. Box 999,
MSIN K6-24,
Richland, WA 99352
e-mail: kriston.brooks@pnnl.gov

Nathan Barrett
Pacific Northwest National Laboratory,
902 Battelle Boulevard,
P.O. Box 999,
MSIN K9-89,
Richland, WA 99352
e-mail: nathan.barrett@pnnl.gov

The pressure vessels needed to store hydrogen for next-generation hydrogen fuel cell vehicles are expected to be a substantial portion of the total system mass, volume, and cost. Gravimetric capacity, volumetric capacity, and cost per kilogram of usable hydrogen are key performance metrics that the U.S. Department of Energy (DOE) uses to determine the viability of hydrogen fuel cell systems. Research and development related to hydrogen storage systems covers a wide range of potential operating conditions, from cryogenic temperatures to high temperatures (above ambient) and low pressure to high pressure. Researchers at PNNL have developed methods for estimating these key pressure vessel characteristics to support on-board hydrogen storage system design and performance evaluation and to support decision-making about DOE hydrogen storage system research investments. This article describes the pressure tank estimation methodology that has been used as a stand-alone calculation and has been incorporated into larger system evaluation tools. The methodology estimates the geometry, mass, and material cost of type I, type III, and type IV pressure vessels based on operating pressure and material strength at the system's operating temperature, using classical thin-wall and thick-wall pressure vessel stress calculations. The geometry, mass, and material cost requirements of the pressure vessel have significant impacts on the total system performance. For example, hydrogen storage materials that can separately achieve a very high hydrogen density can be deemed impractical for use in fuel cell vehicle hydrogen storage systems because the pressure tank containing them is too large, heavy, or expensive. This article describes the design philosophy and analytical process of the tank characteristic estimation methodology, which has been implemented in spreadsheet calculation tools and system-level analysis tools used by DOE researchers. Each of the three tank types (type I, type III, and type IV) uses a different analysis methodology with some common elements. This article also provides examples of implementing the methodology to perform parametric studies of all three pressure vessel types. The goal of this article is to present the methodology in sufficient detail so it can be implemented in other hydrogen fuel cell vehicle design and analysis tools.
[DOI: 10.1115/1.4063884]

1 Introduction

Hydrogen is a viable fuel that could transform the U.S. transportation infrastructure with carbon-free vehicle emissions, but it is difficult to engineer a hydrogen fuel cell vehicle and its storage system that can reasonably compete with a gasoline internal combustion engine or battery electric vehicle on a cost, mass, or volume basis [1–8]. Hydrogen has a higher gravimetric energy density than batteries, diesel, or gasoline, but it is a gas at ambient temperatures. Therefore, hydrogen's key physical problem in comparison to liquid gasoline is its density. Based on the U.S. Department of Energy's (DOE) technical targets, it is estimated that 5.6 kg of hydrogen is needed for a light-duty fuel cell vehicle range

of 300 miles (483 km) [9]. If this mass of hydrogen is held at a pressure expected in the typical home air compressor range of 10 bar (145 psi), the 5.6 kg of hydrogen gas would be approximately 7000 L (about 9 yd^3) in volume. A full-size pickup truck can only carry about 3 yd^3 of heaped material, so a practical passenger car design would need a storage system that holds hydrogen at a much higher density. Due to the complexity of the overall vehicle system and the technical challenge of storing hydrogen in a useful form, numerical tools are required to estimate, design, and evaluate potential on-board hydrogen storage systems.

Hydrogen does not behave like an ideal gas [10–13], so while increasing pressure increases hydrogen gas density, operating in the high-pressure range (e.g., 700 bar) offers diminishing returns on hydrogen gas density. Higher operating pressure also leads to increased pressure vessel wall thickness due to the increased structural loads, leading to heavier pressure vessels and greater overall system weight. Achieving a hydrogen storage density that is high enough to make hydrogen vehicles practical is a significant technical challenge. The pressure tank component of the system can be a dominant factor in determining the gravimetric or volumetric efficiency of a complete system. When performing research on

Table 1 Different tank types and their descriptions

Tank type	Description	Included in methodology?
Type I	Fully metallic pressure vessel	Yes
Type II	Steel pressure vessel with glass fiber composite overwrap	No
Type III	Fully composite overwrap with a metal liner	Yes
Type IV	Fully composite overwrap with a composite liner	Yes
Type V	Fully composite pressure vessel without a liner	No

material-based hydrogen storage technologies, such as metal hydrides, chemical hydrides, or cryo-adsorbent systems, the mass, volume, and cost of the pressure tanks incorporated into each system can drastically affect the viability of the technology [12,14–16]. While research in hydrogen storage media is critical to the technology, an integrated systems analysis is needed to ensure that performance targets are met at the system level.

Early analysis in this area at Pacific Northwest National Laboratory (PNNL) investigated the relationship between internal pressure and system density for a variety of pressure tank materials using spreadsheet calculation methods [17,18]. Variations in size, shape, and pressure tank wall material and temperature were considered to accommodate various hydrogen storage media and evaluate the potential for the various media to meet DOE targets. The research community has identified five different types of tank construction as candidate storage systems with the general characteristics shown in Table 1 [19–21]. The first tanks considered at PNNL were type I (all metal) pressure tanks, and classical thin-walled pressure vessel equations were used to calculate the minimum necessary wall thickness to contain the internal pressure. These informal spreadsheet calculations evolved over time, expanded into Type III and Type IV tanks, and ultimately became the formal methodology that has been used to estimate the overall system mass and volume for metal hydride and cryo-adsorbent-based hydrogen storage systems [14,15]. The calculation methodology is described in this article.

Temperature is another key operational parameter that can be used to modify the effective hydrogen gas density [10,22,23]. Cryo-compressed hydrogen systems can reach system volumetric capacities of 41.8–44.7 kg H_2/m^3 and cryo-adsorbed hydrogen systems can reach 31 kg H_2/m^3 compared to ambient temperature high pressure systems that can achieve only 17.8 kg H_2/m^3 (350 bar) or 25.1 kg H_2/m^3 (700 bar) [24,25]. The tanks evaluated with the methodology all respond differently to reduced temperature. Metal tank materials that behave in a ductile manner, such as austenitic stainless steels, tend to increase strength at reduced temperature. While not accounted for in our study, these potential gains in mass and volume due to improved metal strength and a reduced wall thickness would be offset by the need to add insulation to maintain operating temperatures below ambient conditions. In contrast, some metals become brittle at low temperatures. As a result, these materials such as ferritic stainless steels have been excluded from consideration in the methodology.

Low temperatures can also be challenging for type III composite carbon fiber/metal pressure vessels. Subambient operating temperatures can lead to thermal stresses in the pressure vessel, and thermal expansion/contraction can be an issue because carbon fiber's thermal expansion behavior is the opposite of that of most metals. Because carbon fiber expands rather than contracts at lower temperatures, metal liners can potentially delaminate from a carbon fiber overwrap during changes in temperature and pressure. PNNL analysis of carbon fiber pressure tanks with metal liners under cryogenic operating conditions was initially performed using the ANSYS finite element code [26]. Finite element analysis (FEA) studies in this area (early results are reported in Ref. [17] and additional FEA studies are documented in Ref. [27]) were generalized in the tank estimation methodology as a design rule to estimate carbon fiber and liner wall thickness instead of performing FEA for every case.

Compared to pure hydrogen gas, hydrogen storage materials offer the potential to increase hydrogen density, but the medium requires a controlled temperature and pressure environment to adsorb and release hydrogen [28]. A variety of temperature ranges were considered as research on hydrogen-storage materials was conducted, which required tank estimates to be based on an expanded range of temperature-dependent material properties. PNNL expanded the methodology to estimate tank dimensions, mass, and the cost for material-based hydrogen storage systems in order to calculate system performance values for comparison with DOE targets [11,29].

In 2014, PNNL first released the methodology for public use via spreadsheet tool [30]. The tank estimation methodology spreadsheet tool was created to offer a stand-alone version of the tank characteristic estimation methodology to researchers outside PNNL in the broader hydrogen vehicle research community. The methodology was also integrated into design tools in both MATLAB and VISUAL BASIC [14,15]. This work was sponsored by DOE, and the Excel, MATLAB, and Visual Basic tools that incorporate the tank estimation methodology are available from the HyMARC website.[2] This article describes the latest version of the methodology, as it is currently implemented [31]. The goal of this article is to provide sufficient information that the methodology can be implemented in other hydrogen fuel cell vehicle design and analysis tools. Note that this methodology has been applied to a wide range of hydrogen fuel cell vehicles, including light, medium, and heavy-duty vehicles as well as mining vehicles [32].

1.1 Limitations of the Methodology. It is important to clarify that the tank characteristic methodology is based primarily on the internal pressure structural load and does not consider any other structural loading conditions that are not specified in this article. For example, real hydrogen pressure tanks will need to be attached to a vehicle in some way. The design of the attachment hardware and any stress applied to the pressure vessel from the attachment is not considered. It is assumed that stresses caused by the attachment hardware can be minimized through effective design, but that part of the design problem is not considered in this methodology. Thermal stresses, inertia loads from an automobile crash scenario, and fatigue failure conditions are similarly not considered in this methodology but would need to be considered in a full pressure vessel design for automotive applications. Fatigue is not expected to be a limiting condition for the pressure vessel design from fill and depletion cycles because for a personal automobile the number of refueling cycles is expected to be relatively low (less than 1000). Fatigue may be a more significant issue for attachment hardware, where shock and vibration from the automobile suspension system are transmitted to the pressure vessel.

The overall size of the pressure vessel estimated by this methodology is not limited, but the methodology is intended for pressure vessels that would fit on an automobile, truck, or bus. The methodology can estimate tank characteristics for much larger vessels for stationary use that might be used at a hydrogen generation facility, but gravity loads and seismic loads are not considered. The tank estimates of this methodology have only been compared to pressure vessels of the approximate size and shape needed for vehicle applications, so it is not known how well the methodology would estimate plant-scale pressure vessels.

---

[2]www.hymarc.org/models.html

2 Theoretical Basis for Hydrogen Tank Characteristic Estimation

The goal of the methodology is to be able to estimate the mass, volume, and cost of the material needed to complete a hydrogen storage system. Extensive active research in this area is devoted to identifying materials that absorb or store hydrogen more effectively than simply storing gaseous hydrogen in a pressure vessel. The researchers who are working on hydrogen storage applications need to be able to estimate the basic properties of the pressure tank both with and without hydrogen storage materials to complete the full system evaluation and demonstrate system feasibility relative to performance metrics. The field of storage media options is so broad that a common framework for comparison of drastically different systems is needed. The methodology fills a very specific and critical niche in the larger system design process to provide a screening tool for calculating tank geometry.

While the methodology was created to assist in the development of light-duty automotive technologies, it is also applicable to other mobile applications (forklifts, trucks, busses, ships, mining equipment, trains, etc.) and stationary applications because it is based on fundamental engineering mechanics analysis methods. The type I and type IV tank estimates are generally applicable to all pressure vessels. The type III tank methodology is applicable to general use, but the tank estimate assumes the tank will experience a cryogenic fueling and depletion cycle which is not a concern in all pressure tank applications.

2.1 Methodology Applied to a Thin-Walled Spherical Type I Tank.

Practical pressure tank geometry is one of the complicating factors in tank characteristic estimation. Car designers have limited space to fit pressure tanks around other features that are competing for space. The methodology estimates tank characteristics for cylindrical pressure vessels with input from the user. The case of a spherical thin-walled type I pressure vessel is a convenient place to begin the discussion because there are ultimately only two parameters to define the spherical vessel, internal radius (R) and wall thickness (t_{wall}).

All hydrogen storage tanks must hold a volume of material, V, which is dictated by the efficiencies and requirements of the system. If we assume the volume is contained within a perfect sphere, the only geometric variable required to define the internal tank geometry is R. The equation for the volume of a sphere is

$$V = \frac{4}{3}\pi R^3 \qquad (1)$$

Rewritten in terms of the radius R

$$R = \sqrt[3]{\frac{3V}{4\pi}} \qquad (2)$$

Equations (1) and (2) are both important because, depending on the analyst's perspective, either R or V might be the independent variable. A car designer might only have room for a spherical pressure tank of radius R, which limits the volume of hydrogen storage space to V. Limiting V would affect the maximum range of a vehicle between refueling stops. A materials scientist might be evaluating the potential of a candidate system to meet performance goals, and geometric constraints might be less important than the potential system's gravimetric efficiency (hydrogen mass per kilogram of system mass). Whatever the perspective or application, R is the variable that is used as an input to determine the stress state and wall thickness.

The stress state in the walls of a thin-walled spherical pressure vessel is relatively simple. In the thin-walled assumption, the radial stress is approximately zero and the axial and hoop stresses are as follows [33]:

$$\sigma_{axial} = \sigma_{hoop} = \frac{PR}{2t_{wall}} \qquad (3)$$

where P is the internal pressure, R is the internal radius, and t_{wall} is the wall thickness. A simple approach to estimating the minimum t_{wall} is to set the axial and hoop stress equal to the ductile metal tank material yield strength value (Sy), which implies that the stress state in this idealized pressure tank wall will reach, but not exceed, yield. A safety factor (F) can be applied to ensure that the material completely avoids the onset of plastic deformation. Equation (4) shows Eq. (3) rearranged to solve for t_{wall}, replacing the stress terms with Sy, and including the safety factor, F

$$t_{wall} = \frac{FPR}{2Sy} \qquad (4)$$

Once the wall thickness is calculated, the mass of the empty spherical tank can be calculated by multiplying the surface area of the sphere by the thickness (to calculate tank material volume) and then multiplying the material volume by the material density, as expressed in Eq. (5). The mass (M) is directly proportional to t_{wall} and to material density (ρ)

$$M = 4\pi R^2 t_{wall} \rho \qquad (5)$$

Once the mass of the tank is known, the cost is calculated by multiplying mass by cost per unit mass of materials of construction. The cost estimate only considers the tank's raw material cost. It does not attempt to include valves, fittings, or other necessary hardware, nor does it consider the cost of manufacturing. The end product of this calculation is an estimate of the tank mass and its material cost, especially as a comparison tool for alternate materials. Precise tank design and cost estimation for a prototype tank are beyond the methodology's intended purpose.

It is worth noting a few things about this basic example of a spherical pressure vessel. Combining Eqs. (4) and (5) yield Eq. (6), which shows the key relationships of parameters to tank mass. Mass is directly proportional to density, pressure, and safety factor, which means each of those three parameters carries equal weight. Mass is proportional to radius cubed, which indicates that the tank radius parameter is much more impactful than the other parameters in the numerator. Being in the denominator, Sy has an inverse relationship to tank mass, such that relatively stronger materials produce relatively lower tank mass. A hidden parameter is temperature, which can significantly affect Sy, with higher temperatures corresponding to lower Sy and higher tank mass and lower temperatures corresponding to higher Sy and lower tank mass. Some materials have a drastic drop-off in strength that makes them unsuitable for use above certain temperature thresholds

$$M = \frac{4\pi R^3 \rho FP}{2Sy} \qquad (6)$$

2.2 Tank Estimation Methodology Base Geometry.

The first technical challenge in estimating pressure tank characteristics is defining the base geometry. The analysis philosophy is to establish the internal geometry of the pressure tank and then calculate the pressure vessel wall structure needed to surround and contain the pressure inside. It can be thought of as a geometry problem, followed by a structural design problem. The basic geometry assumed for the pressure tank is shown in Fig. 1, a cylindrical tank with a constant wall thickness having hemispherical end caps or semi-elliptical end caps.

Different users have different needs in terms of the geometry problem. Materials researchers might be content to assume an L/D ratio of 2 for all their tank estimates. Researchers involved in automotive design might instead be concerned with the geometry envelop of a gasoline fuel tank or the space of a trunk to consider where a hydrogen fuel tank could fit within an existing car design.
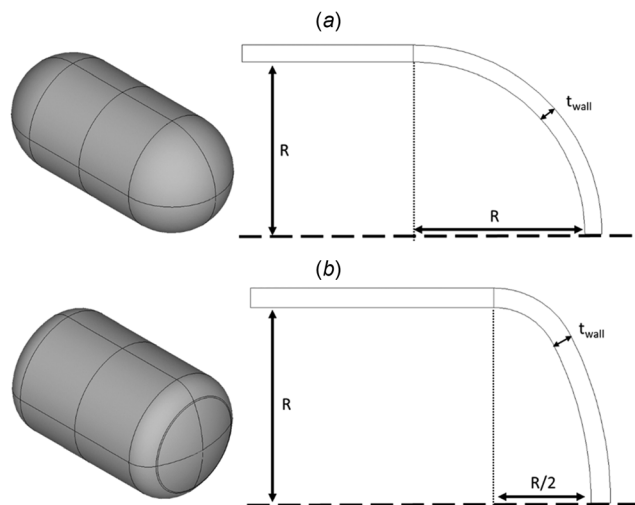
Fig. 1 Quarter section of the basic pressure vessel geometry used in this methodology. (*a*) Hemispherical end caps were the only option in previous revisions. (*b*) Semi-elliptical end caps are now also included. The wall thickness of the tank (t_{wall}) is calculated based on the geometric inputs internal radius (*R*), internal length (*L*), internal volume (*V*), and additional inputs like pressure and temperature.

The methodology was developed to meet the needs of both kinds of users.

The methodology uses the same general process outlined above in the spherical Type I tank example to estimate tank mass for type I, type III, and type IV cylindrical pressure tanks. It is expected that cylindrical tanks with external length/diameter ratio (L/D) greater than 2 are of primary interest for automotive applications because they are easier to incorporate into an automobile design without impinging on the passenger compartment, trunk space, or other key functional components of an automobile. L (internal length), R (internal radius), and V (internal volume) are the three parameters that define the geometry of the pressure tank estimates according to Eq. (7) for the hemispherical end caps and Eq. (8) for the semi-elliptical end cap option. Note that only two of the three variables in Eqs. (7) and (8) are used as inputs. Any two of L, R, and V can be used as the independent variables in Eqs. (7) and (8), resulting in the third variable becoming dependent. V is often the starting point because the hydrogen storage capacity of a proposed storage medium is known because it is a chief concern for material scientists, and V must be set with knowledge of material storage capability to achieve the necessary driving range of the vehicle. For automobile design applications, R and L may instead be more important when the tank is being considered to fit within an available space. The methodology is coded to accept any two of the three geometry inputs to accommodate various uses

$$(\text{for hemispherical end caps})V = \frac{4}{3}\pi R^3 + (L - 2R)\pi R^2 \quad (7)$$

$$(\text{for semi elliptical end caps})V = \frac{2}{3}\pi R^3 + (L - R)\pi R^2 \quad (8)$$

The first calculation step in the methodology is to determine R, L, or V from the other two input values. If R and L are both specified by the user, V is calculated according to Eqs. (7) or (8), and any input value for V is treated as a volume goal. If either R or L is specified as zero by the user, V is treated as an input variable and used directly in Eqs. (7) or (8) to determine the missing value. When either V and L or V and R are provided as inputs, solving Eqs. (7) or (8) for the missing variable is more difficult because the equation has several roots. A Newton–Raphson iterative linear approximation process is used to find the appropriate root to solve for R or L. Enough iterations are

incorporated into this methodology to provide an accurate result for the remaining unknown variable, and flags are incorporated into the results that indicate to the user if convergence has not been achieved. In the situation where convergence is not achieved, the flags indicate to the user which parameters are likely resulting in unrealistic tank geometry, and how they can be corrected. Additionally, checks are made for inconsistent geometry values. For example, $L < 2R$ is invalid in Eq. (7) because it breaks the assumption of a cylindrical pressure vessel.

Of the three geometry parameters, R is critical for the stress calculations, as will be shown in Secs. 2.3–2.5. L is needed for the mass calculation and the total geometry definition but does not directly affect the stress in the pressure vessel walls or the calculation of wall thickness. V is only needed to compare against design targets, or to derive R or L.

2.3 Estimation Methodology for Type I Pressure Tanks. Type I tanks are metal pressure vessels made of a single material. The type I tank estimate of wall thickness uses an equation that is similar to Eq. (4). The only difference is a factor of two in the denominator, which is because the hoop stress in a thin-walled cylinder is twice as high as that in a sphere of the same radius [33]. Equation (9) calculates the necessary wall thickness to support the hoop stress, which is twice the value of the axial stress. This is equivalent to designing the pressure vessel based on a stress intensity design criterion, with stress intensity defined as the maximum difference in principal stresses in a three-dimensional stress state. American Society of Mechanical Engineers Boiler and Pressure Vessel Code (ASME BPVC) uses stress intensity limits in Section III, Division 1, Subsection NB [34] for nuclear power plant components, although it is not the only stress limits used in ASME BPVC. In Section VIII, Division 2 the ASME BPVC defines stress limits based on the von Mises failure criterion, although requirements on materials, design, and nondestructive examination are more rigorous than in Division 1 [7]. For Type I tanks, the methodology considers both the stress intensity criteria for thin-walled pressure vessels and von Mises criteria for thick-walled pressure vessels, as described in the following paragraphs.

In the case of a thin-walled cylinder, the normal stress is zero, so the maximum stress intensity is the maximum of the hoop or axial stress

$$t_{\text{wall}} = \frac{FPR}{Sd} \quad (9)$$

The methodology uses two design criteria for type I tanks: a proof load and a burst load. The proof load is the maximum pressure that can be applied to a system before permanent deformation begins. The burst load is the maximum pressure the system can hold before the pressure boundary fails. The proof load is 1.5 times the operating pressure. The burst load is 2.25 times the operating pressure [27]. The proof load design criterion uses the material yield strength as the design strength. The burst load uses the material ultimate strength as the design strength. The methodology has realistic, temperature-dependent yield and ultimate strength data defined for each material and looks up the strength values for the specified operating temperature. By using actual material yield and ultimate strength values instead of more limiting ASME BPVC allowable stress values, such as those defined in ASME BPVC Section II, Part D [34], the calculations performed in the methodology are able to provide less conservative estimates for tank mass and geometry. The gravimetric efficiency targets of on-board hydrogen storage systems are so demanding that the lightest possible tanks that can be demonstrated to meet safety requirements are required. The determination of the limiting load (proof or burst load) is represented in Eq. (10), which is used to calculate the minimum necessary wall thickness, t_{wall}, which is the starting point for further refinement

$$t_{\text{wall}} = \text{Max}\left(\frac{1.5PR}{Sy}, \frac{2.25PR}{Su}\right) \quad (10)$$

Equation (10) usually offers a reasonable estimate of tank mass, but it is possible that the calculated wall thickness will be too thick to use the thin-walled pressure vessel assumption. The difference between the thin-wall case and the thick-wall case is that the radial component of stress from the internal pressure can be ignored (assumed to equal zero) in the former and must be accounted for in the latter. The thin-walled assumption is generally considered valid when the ratio of the radius to the wall thickness is 10 or greater [35]. Instead of introducing logic to stop the calculation if the thin-walled assumption is appropriate, the methodology always proceeds with three iteration cycles to refine the wall-thickness estimate from Eq. (10) based on the most limiting three-dimensional stress state in the pressure vessel wall. The thick-walled pressure vessel assumption and the von Mises yield criterion are used to drive the wall thickness toward a value that equals the proof stress limit or the burst stress limit, whichever is most limiting. This process is appropriate for thin- or thick-walled pressure vessels, and in some cases leads to a reduction in mass relative to the initial estimate. Three iteration cycles are typically sufficient to achieve a reasonable tank estimate, but in rare cases where the walls are extremely thick there may still be some residual error between the stress state and the target stress. The methodology reports the amount of error, and the user can decide whether to keep the estimate or reject it. Cases that fall into this category tend to be impractically heavy—an indication that the selected pressure vessel wall material is not strong enough for the temperature and pressure demands.

For example, consider the input parameters of a pressure tank to be 25 °C, 250 bar, 81 cm (L), 22.5 cm (R), estimated 105,000 cm³ (V), and 6061-T6 aluminum material, which has yield strength of 2,806 bar and an ultimate strength of 3085 bar. (Note that bar is commonly used as the primary pressure unit in this research area, and this article uses bar for stress calculations for consistency, where 1 bar = 0.1 MPa). The first estimate of t_{wall} is 4.103 cm, which is based on the thin-wall pressure vessel assumption and Eq. (10). The methodology then calculates the von Mises stress (σ_{eqv}) at the proof load and burst load based on the thick-walled pressure vessel assumptions and Eq. (11), where σ_1, σ_2, and σ_3, are the principal stresses that align with hoop stress, axial stress, and radial stress, respectively,

$$\sigma_{\text{eqv}} = \sqrt{\frac{(\sigma_1 - \sigma_2)^2 + (\sigma_2 - \sigma_3)^2 + (\sigma_3 - \sigma_1)^2}{2}} \qquad (11)$$

For this example, the von Mises stress at the proof load is 2315 bar (Sy is 2,806 bar) and the von Mises stress at the burst load is 3472 bar (ultimate strength Su is 3085 bar). The burst load exceeds the ultimate strength by about 11%, which indicates that the wall thickness must be increased to avoid a failure of the pressure tank under burst loading conditions. The iterative process increases the initial wall-thickness estimate by 11% and calculates an updated von Mises stress, which at the end of this cycle is about 3% higher than the ultimate strength. The second iteration cycle increases the wall thickness by 3% and determines the von Mises stress is still 0.6% too high. The third and final iteration increases the wall thickness by 0.6% and determines the von Mises stress is still 0.14% too high. The iteration ends with an estimated 0.14% of remaining error in the wall thickness, but the error in wall thickness is approximately equal to the error in tank mass, so a 0.14% error is acceptably small for the purposes of estimating tank characteristics. Through this iterative process the wall thickness increased from its initial estimate of 4.103 cm to 4.693 cm, an increase of 13.7%, which is a significant fraction of the tank mass.

A finite element model was developed in ANSYS R19.0 to calculate the overall stress state for type I tank estimates to validate the methodology. The model is used here to illustrate how the von Mises refinement steps in the methodology drive the design to an acceptable stress state. The three-dimensional model assumes elastic material behavior and uses second-order tetrahedrons with approximately three elements through the wall thickness. A brief
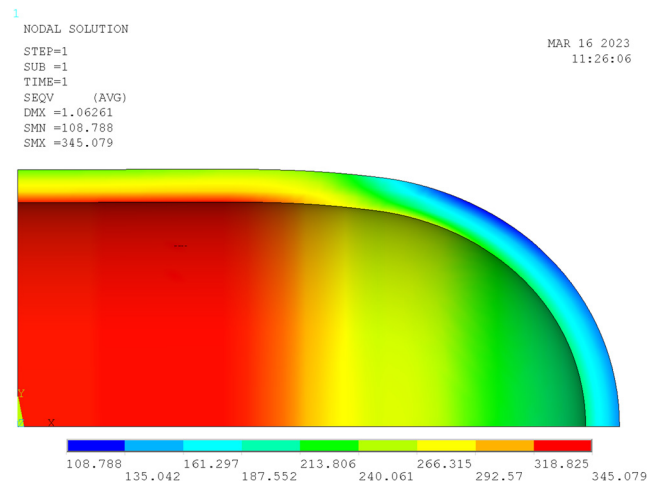

Fig. 2 Finite element model of the burst pressure load case using an initial wall-thickness estimate

mesh sensitivity study was conducted to confirm the element size does not have a significant effect on the value of the peak von Mises stress. Figure 2 shows the von Mises stress contours in units of megapascals (MPa) for the burst load pressure and the initial methodology wall-thickness estimate (which is based on thin-wall pressure vessel theory). The finite element model calculates a peak (nodal) von Mises stress of 345.1 MPa (3451 bar) while the methodology estimates the peak von Mises stress to be 3442 bar, a difference of less than 1%. Note that the peak stress is on the inside surface of the pressure tank and the stress decreases through the wall to the outer surface. The average stress through the limiting cross section is approximately 300 MPa (3000 bar), which is above the yield strength but below the ultimate strength. The finite element model assumes the aluminum is elastic and calculates a linear structural response to the applied pressure. The methodology assumes this stress state is not acceptable and increases the wall thickness to avoid it.

Figure 3 shows the von Mises stress contours in units of megapascals for the burst load pressure and the final methodology wall-thickness estimate. The finite element model calculates a peak (nodal) von Mises stress of 311.3 MPa (3183 bar), while the methodology estimates the peak von Mises stress to be 3089 bar, a difference of under 1%. The average von Mises stress through the
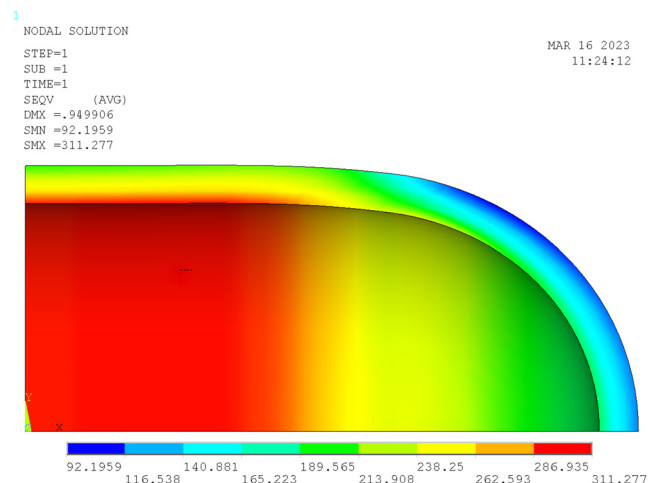

Fig. 3 Burst load with updated wall thickness. The thin-wall pressure vessel estimate calculated a wall thickness that was too thin. The thick-wall pressure vessel estimate increases the wall thickness and reduces peak stress to an acceptable value.

Table 2 Material properties at 22 °C for materials included in the methodology

	Yield strength (bar)	Ultimate strength (bar)	Mass density (kg/cm^3)
6061 T-6 aluminum	2,811	3,095	0.0027
A2618 aluminum	3,720	4,410	0.0027
A4032 aluminum	3,150	3,803	0.0027
AL-MS89 aluminum	3,848	4,594	0.0027
NASA-2219 aluminum	3,455	4,558	0.0028
NASA-380 aluminum	2,350	2,770	0.0027
316 stainless steel	2,874	5,897	0.0080
4130 chromoly steel	6,690	7,240	0.0077
4340 alloy steel	4,069	7,919	0.0079
A289 stainless teel	5,465	10,000	0.0078
XM-19 Nitronic® 50 stainless steel	5,388	8,581	0.0079
A286 nickel alloy	7,026	10,069	0.0079

limiting section is about 2700 bar, which is slightly lower than the yield strength of 2806 bar. This model assumes linear elastic behavior, but the calculated results suggest the plastic strains could occur in the red and orange contours. As noted above, this stress state is about 0.14% away from the target stress state, so it is a good illustration of the stress state the methodology is attempting to achieve in the burst test scenario. Recall that this load case applies a 2.25 multiplier on the operating pressure, representing an extreme overpressure event. This load case does not represent normal operating conditions and is meant to assure safety during over-pressure events.

Note that the pill-shaped geometry simplifies the geometry at the ends of the cylinder as perfect hemispheres. The hemispherical ends have significantly lower stress in Figs. 2 and 3 than the cylindrical region, where the most limiting stresses are located. The low stress locations indicate that the shape could be optimized to reduce the weight of the pressure tank. Real pressure tanks have more complicated geometry at the ends, including openings for piping and valves. Those features would add to the local stress demands of the design. The relatively low stress state in the hemispherical end cap geometry provides a margin to optimize the end cap geometry and account for the necessary fittings within the total mass estimate. Fine details of the design, like fittings, are outside the scope of the estimation methodology. Comparisons of tank estimates from this methodology to existing tank designs have demonstrated that the methodology makes reasonably accurate weight predictions of tanks regardless of end cap geometry [27].

The methodology offers a second option for end cap geometry, 2:1 semi-elliptical. There are many practical design options for the ends of cylindrical pressure vessels, but the 2:1 semi-elliptical end is commonly used in pressure tank design and remains efficient in terms of tank mass. This change in end cap geometry only modifies the internal volume of the pressure tank and the calculation of the tank's mass. The wall thickness in the semi-elliptical end cap is equal to the wall thickness in the cylindrical shell section of the pressure tank, which is the same as that in the hemispherical end cap case. However, in the hemispherical end cap case wall thickness is known to be greater than necessary (adding conservatism to the tank estimate), while in the 2:1 semi-elliptical case the end caps are expected to be appropriately sized. ASME BPVC Section VIII, Division I, Subsections UG-27 and UG-32 provide guidance for determining the minimum necessary thickness for internally pressurized pressure vessel cylinders and end caps, respectively. In all cases, the minimum thickness of the 2:1 semi-elliptical end cap does not exceed the wall thickness of the cylinder. As a result, the assumption of constant thickness of the end cap and vessel cylinder is reasonable.

The material properties of the tank wall material are a key part of the tank characteristic estimation. The yield strength, ultimate strength, and density all affect the ultimate calculation of tank mass. The estimation methodology can implement any material property data that is provided. All of the tools that use this methodology have a built-in library of material data that was assembled from open

source material. Table 2 summarizes the material data at room temperature that is built into the spreadsheet tool implementation of the methodology. The full temperature-dependent material property sets (from cryogenic temperatures up to approximately 250 °C) can be found in the spreadsheet tool [31].

To complete the type I tank estimate, the wall thickness calculated according to Eq. (10) or subsequent von Mises stress refinement iterations is used with the base geometry calculation (Eqs. (7) or (8), depending on choice of end caps) to calculate the outer envelope and total volume of the tank. The tank wall volume is equal to the inner volume (Eqs. (7) or (8)) subtracted from the total volume. It follows that the mass of the tank wall is the volume of the tank wall times the material density, and the material cost of the tank is the tank mass multiplied by the price per kg of tank wall material.

2.4 Type IV Tanks. A type IV tank has carbon fiber fully wrapped around a high-density polyethylene (HDPE) liner. Type IV tanks are discussed next because while type III tank methodology is very similar to that for the type IV tank, the type III tank has the complexity of an added aluminum liner that contributes structural support. In contrast, the HDPE liner carries no structural load and is only present as a barrier layer to prevent hydrogen from passing through the carbon fiber. Liner thickness is an input that can be set to any thickness; its only effect on the stress state is to increase the internal radius of the carbon fiber layer. The carbon fiber wall thickness is calculated according to Eq. (12), which is a modified version of Eq. (9). It is essentially a thin-walled pressure vessel with adjustments made to account for carbon fiber material and uncertainties related to its structural performance. Fiber translation efficiency (K_{fte}) is introduced as a parameter to represent the difference between theoretical and practically achievable carbon fiber strength. Sd in Eq. (12) is the design strength of the carbon fiber composite wall in the hoop direction, assuming a laminate stack that aligns two-thirds of the fibers in the hoop direction and one-third of the fibers in the axial direction. Carbon fiber pressure tanks are typically wound with carbon fiber tows at angles that produce crossing helical patterns and hoop windings. The composite material strength typically approaches the ideal 1/3, 2/3 distribution, but the fiber layup directions do not precisely align with the 0 deg and 90 deg directions. The methodology assumes that the composite is comprised of many alternating layers carbon fiber laminate that approximates an ideal 1/3, 2/3 distribution

$$t_{\text{wall}} = \frac{FPR}{K_{\text{fte}}Sd} \tag{12}$$

The default value for K_{fte} is 80%. This value was generally used in tank mass estimates at PNNL because it led to reasonable agreement with commercial examples of type IV tanks. When the methodology was being developed, available type IV pressure tank burst data suggested K$_{fte}$ should be in the 70% to 85% range. In one example in the literature, an ABAQUS finite element analysis compares to burst

test data of Type IV tanks and estimates the failure strain is 85% less than the material data sheet values of Toray's technical data sheet for T700 composite [36]. This factor was incorporated into the methodology because the tank wall-thickness estimate is based on an ideal distribution of carbon fiber in the hoop and axial directions, without considering winding angles. This factor offers a simple way to account for imperfect manufacturing or design methods. The effect of translation efficiency can be eliminated completely by setting it equal to 100%.

The design strength of carbon fiber laminate in the hoop direction is assumed to be 15,306 bar. This strength value is based on a 60% fiber volume fraction and a two-thirds distribution of fibers in the hoop direction. This homogenized design strength represents an individual composite layer strength of about 22,300 bar. One example that meets this composite strength value is Toray T700S (per the manufacturer's technical data sheet [37]). This design strength (Sd) is not a variable that is intended to be changed during standard use of the methodology for simplicity, but it can always be customized to accommodate other fiber strengths, fiber volume fractions, or fiber orientation angles based on user needs. An easier way to effectively modify the composite design strength is by changing the K_{fte} value in Eq. (12), which is designated in the spreadsheet tool, and other implementations of the methodology as a user-defined input parameter. Similarly, the safety factor (F) is fixed at 2.25, but larger or smaller safety factors can be achieved using the K_{fte} value. Note that estimates are not necessarily aligned with current consensus standards or regulations, but the K_{fte} input parameter can be used to account for safety factors, design standards, or experimentally observed composite strengths as necessary to meet the objectives of the tank estimation study.

Equation (12) was formulated for generic implementation in the methodology at a time when the practical limits and necessary rules of carbon fiber pressure vessel design remained uncertain. The methodology was found to provide reasonable estimates of type IV pressure vessels, and that was sufficient for the intended use of the methodology. Future implementations of this methodology could simplify Eq. (12) by removing the K_{fte} input parameter and revising Sd to be an experimentally determined design strength based on specific carbon fiber and resin material properties, winding angles or layup orientations, and industry experience applying the composite material to pressure vessels. The K_{fte} and Sd parameters represent an efficiency parameter and a theoretical material strength, respectively, and together they could be replaced by a net practical strength value if that value happens to be known to the user. Equation (12) calculates the composite wall thickness as a single value, but carbon fiber laminate pressure vessels are built in discrete layers. Each layer of carbon fiber laminate is assumed to be 0.9144 mm thick, and the methodology rounds up the real value of thickness calculated in Eq. (12) to the next integer multiple of layer thickness, with a minimum of three layers. The 0.9144 mm thickness is based on a specific tow size, but smaller layer heights could be used to achieve an equivalent, or more optimized wall thickness. Similarly, details of winding angles are not considered. It is assumed that a set of specifications for a type IV pressure vessel can be achieved with the number of layers estimated by the methodology, but a detailed pressure vessel design effort might conclude that additional layers are needed to accommodate practical winding angle limitations. The potential need to increase laminate layers above the estimate will have the largest effect on the three-layer minimum cases because adding a fourth layer of laminate causes a 33% increase in thickness. If there are 10 layers of laminate, adding an eleventh layer only causes a 10% increase. Comparisons of Type IV mass estimates to existing type IV tank designs agreed within ±10% [27], which is the desired range of accuracy for this tool. The error is potentially larger than 10% when the layer thickness is small, but a user can account for this by adjusting K_{fte} to match examples that are in the size and pressure range of interest, applying a penalty factor outside of the estimation methodology parameters, or unlocking the spreadsheet to modify the composite design strength or minimum layer thickness. This methodology is intended to estimate carbon fiber tank characteristics, rather than be a tool to perform detailed carbon fiber tank design. It is envisioned that different design approaches, like netting analyses or sophisticated computer-aided design, would be used by a tank designer to define an optimized design. This methodology provides a first estimate of the characteristics of the optimized design.

Temperature is not an input to the type IV tank estimate because the operating temperature limits depend on the properties of the matrix material. Some epoxy resins are limited to 100 °C, while others can match the temperature range of metal tanks. This is left to the user to be sure that the pairing of carbon fiber and epoxy matches the demands of the tank application.

While the type IV calculation always provides an estimate of tank mass and geometry, an important check is made by the spreadsheet and in other implementations of the methodology to confirm that the thin-walled pressure vessel basis of the calculation is appropriate. For an accurate type IV tank estimate the final R/t_{wall} ratio should be greater than 10. If the R/t_{wall} ratio is not greater than 10, the pressure vessel estimate is outside the normal expected range of application and the estimate should be compared to existing pressure vessels that have a similar geometry and pressure rating to confirm that the estimate is reasonable. A warning flag is provided when R/t_{wall} is less than 10. The K_{fte} parameter offers an easy way to adjust the calculations to match existing examples in narrow size and pressure ranges if such calibration is needed.

The type IV tank estimate is completed by calculating the volumes of the carbon fiber overwrap and the liner that surrounds the pressure vessel internal volume. Equations (7) or (8) are used, depending on the choice of end caps, to calculate the total outer volume of the tank (with radius R equal to internal radius + liner thickness + t_{wall}), outer volume of the liner (with radius R equal to internal radius + liner thickness), and inner volume of the tank (with radius R equal to internal radius). The volume of carbon fiber material is the outer volume of the carbon fiber minus the outer volume of the liner. The volume of HDPE liner material is the outer liner volume minus the inner volume of the tank. The mass of carbon fiber composite material and HDPE liner material are calculated from the material volumes, and material costs are calculated from the masses.

2.5 Type III Tanks. The type III estimates provided by the methodology produce the mass and geometry of a tank composed of an aluminum liner and a carbon fiber overwrap. Unlike the types I and IV pressure tank estimations, which are valid for a wide range of temperatures, the type III estimation is formulated specifically for a cryogenic tank system whose operating cycle reaches 80 Kelvin or lower. The assumed cryogenic operating cycle goes from a minimum of 80 K at full hydrogen up to 140 K at the empty state. The refueling steps of the cycle are evaluated with a potential overpressure of +25% above operating pressure at a relatively warm 180 K. These operational parameters and the type III tank estimation feature were developed to support DOE research of cryo-adsorbent systems [27]. The tank system operating cycle drives a number of assumptions and design criteria. One of them is that the tank will be manufactured at room temperature, and then be cooled to cryogenic temperatures for service. Additionally, the temperature will cycle through a fueling, depletion, and refueling cycle under normal operation. The difference in the coefficient of thermal expansion is a major consideration for the structural design of type III tanks for this kind of application.

Aside from the standard tank geometry inputs (R, L, V), operating pressure (P) and fiber translation efficiency (K_{fte}) are the only inputs to the calculation. The same considerations of K_{fte} discussed in the type IV tank section apply. As was the case for the type IV tank estimation, the K_{fte} value of 80% is recommended but setting it to 100% effectively removes the factor from the calculation.

The key design feature of the type III case is the aluminum liner. The thickness of the aluminum liner is calculated to be a certain size based on FEA of the thermal expansion of carbon-fiber-wrapped liners during the anticipated cryogenic operation and refueling

cycle. The coefficient of thermal expansion (CTE) of carbon fiber laminate is the opposite of aluminum (and most metals) because it expands when the temperature decreases, while aluminum and most metals contract. For examples, see Ref. [35], where the CTE is listed as negative, and [34] which identifies CTE for various common metals. This affects the load-sharing capability of the mixed-material pressure tank. A small amount of plastic deformation is acceptable in the liner when the pressure tank is initialized (a process expected to be completed under controlled, factory conditions), but to avoid fatigue problems no further plastic deformation is allowed throughout the operating life of the cryogenic tank.

The finite element study performed on many different sizes and operating pressures identified a simple way to size the aluminum ring to avoid cycling plastic deformation during the thermal cycle. The liner is sized to support 21% of the pressure load as defined in Eq. (13), and the composite is sized to carry the rest. The 21% factor was selected based on a parametric study of the Type III cryogenic tank section finite element model that is discussed in Refs. [17] and [38]. The parametric study covered operating pressures up to 300 bar and an internal radius up to 30 cm and concluded that a 21% load-sharing fraction consistently resulted in a reasonable liner and overwrap design. Equation (13) is very similar to Eq. (8) because it is based on the thin-wall pressure vessel stress state. In Eq. (13), Sd is the ultimate strength of the aluminum liner at room temperature. Equation (13) is based on the room temperature liner properties because an initial room temperature pressurization is expected to be used to put a small amount of plastic deformation into the liner, which is needed to maintain contact between the liner and the carbon fiber overwrap throughout the cryogenic temperature cycle of normal operation. No further plastic deformation is expected to occur during the service life of the tank

$$t_{\text{liner}} = 0.21 \times \frac{2.25PR}{Sd} \qquad (13)$$

With Eq. (13) defining the liner thickness, the rest of the calculation is performed in a manner similar to that performed for the type IV tanks, with the liner thickness adding to the inner radius of the carbon fiber overwrap. One difference from the type IV calculation is that two tank estimates are made: one each for the upper bound and lower bound cases. The upper bound case assumes the liner is not effective in carrying any amount of the pressure load, while the lower bound assumes the liner carries 21% of the load, consistent with Eq. (13). The lower bound case is the best estimate case, while the upper bound case provides a conservative upper bound for tank mass. The difference between the two cases is how much carbon fiber the liner effectively replaces.

The volume, mass, and material cost of the carbon fiber composite and the aluminum liner are calculated in the same manner as the type IV case, as described in Sec. 2.4. The main differences are that the aluminum liner is relatively heavier than the HDPE liner assumed in the type IV tank and the fact that upper bound and lower bound estimates are made in the type III tank calculation.

For all tank types, this methodology provides estimates of the mass and geometry of hydrogen pressure tanks. The type III tank is the type that is expected to need the most detailed design work, especially considering the unique thermal expansion challenges that are expected. The 21% load sharing at the foundation of the analysis is believed to be reasonable based on FEA, but this has not been confirmed with bench-scale or prototype testing. The methodology is intended to offer a good starting point for a tank designer, and the calculation of upper and lower bound cases in the type III tank estimate reflects that goal.

3 Implementation Examples

The value of this analysis methodology is the ability it affords to explore the pressure vessel design space. This can be done to evaluate the viability of hydrogen storage systems in general, or for more vehicle-specific applications. Researchers at PNNL used this methodology to help understand the challenge of meeting DOE target goals, such as gravimetric efficiency, volumetric efficiency, and cost targets, and evaluating new technology options.

An example of using this methodology to evaluate type I tank options is summarized in Table 2. The same input parameters and geometry specifications were used for all twelve metal materials defined. The relatively high pressure of 250 bar has a significant effect on the design space. In most cases, the initial von Mises assessment determined that the thin-walled pressure vessel assumption did not apply because the R/t_{wall} ratio was less than 10. The three von Mises refinement iterations drove the wall thickness higher, and the remaining error between the optimal wall thickness and the final estimated wall thickness is less than 1%. For this kind of estimate, error below 1% still offers a reasonable estimate of the size, mass, and cost of the pressure tank, but the calculated von Mises stress at the most limiting point is still above the design limits.

In this example, the specialty steels (e.g., 4130 steel, 4340 steel, and XM-19 and 4130 chromoly) are strong enough to withstand the pressure and still be classified as a thin-walled pressure vessel. The von Mises refinement steps reduced the wall thickness from the initial thin-walled estimate and converged to approximately zero error. The aluminum tank designs of Al-MS89 and NASA-2219 are superior to all the others in terms of mass but no cost is available for these materials. The 4130 chromoly tank design is heavier than these tanks by approximately 50% but is the lowest cost tank of those with available material costs. The 316 stainless steel and 6061 aluminum tanks both look like undesirable choices because of their cost and mass. Note that many of the materials in Table 2 are marked N/A, which indicates that no raw material cost is available. With the cost of materials changing over time and the cost of fabrication having a potentially larger impact on the total tank cost than the raw material cost, the cost estimate from the methodology is primarily intended to study trends and relative rankings, rather than estimating total system cost. For example, the 316 stainless steel tank is both the heaviest and most expensive tank in Table 2, which suggests all the other materials are more favorable options but quantifying the precise difference in cost between a 316 stainless steel tank and 6061 aluminum tank requires a more sophisticated analysis than this methodology can provide.

In a second example application, the effect of operating pressure on a type III cryo-adsorbent system is studied. The tank must have a volume capacity of 105,000 cm^3 and an internal radius of 22.5 cm. The pressure is varied up to 300 bar, which is the highest pressure for which this analysis method was independently evaluated using FEA and is the recommended limit of application of this analysis methodology for type III tanks. This type of tank cycles between 160 K and 80 K during its operating cycle. Table 3 shows the increase in composite layers, total mass, and material cost with increased pressure. The inner geometry remains fixed, but the outer geometry increases because a thicker wall is needed to support the higher pressure. While minimizing P minimizes t_{liner} (see Eq. (13)) and thus reduces the cost of the tank, lower pressures also reduce the adsorbent hydrogen storage capacity. In contrast, with higher pressures, the advantage of cryo-adsorbents over cryo-compression begins to disappear because of increased compression energy and increased storage vessel costs. As a result, there is a balance between

Table 3 Type III pressure variation example summary

Operating pressure (bar)	Composite layers	Total tank mass (kg)	Total material cost (USD)
50	3	14.5	$201
100	4	17.6	$261
150	6	26.6	$398
200	8	35.9	$540
250	10	45.3	$685
300	12	55.0	$834

Table 4 Type IV radius variation example summary

Inner radius (cm)	Outer diameter (cm)	Outer length (cm)	Composite cost (USD)	Total tank mass (kg)
17.5	37.4	123.2	$612	24.3
20.0	42.8	99.7	$695	26.4
22.5	48.0	84.0	$727	26.9
25.0	53.2	73.3	$772	27.9

the functional properties of the cryo-adsorbent media and the cost of the storage vessel.

For cryo-adsorbent systems, recent research indicates that 100 bar operating pressure is a favorable pressure to maximize cryo-adsorbent gravimetric efficiency [39]. This is also an example of research that used the methodology, and it is identified in this paper as the *H2 Tank Mass and Cost Estimator*. The paper used type I pressure tanks in its parametric studies but noted that the same studies could also be done for type III tanks.

An example of type IV calculations is shown in Table 4. In this case, the operating pressure was fixed at 250 bar and the internal volume requirement was fixed at 105,000 cm^3. The internal radius was varied from 17.5 cm to 25 cm. For the volume target, 25 cm is close to the practical limit of interest. As Table 4 shows, the ratio of the outer length to the outer diameter is about 1.4. The tank estimation logic begins to break down when the L/D ratio reaches 1, which is a spherical shape. The methodology adds a flag to alert the user when the geometry inputs are inconsistent with the assumption of a cylindrical pressure vessel.

The results in Table 4 show that the smaller radius is most effective (i.e., it has the lowest total tank mass), but in a practical automotive application, the vehicle design will place constraints on the available space. The 20 and 22.5 cm radius cases are similar in mass and cost. The 25 cm radius case is approaching an L/D ratio of 1, so it is getting close to spherical in shape, which may be more challenging to manufacture. Note that this case fixes the volume, pressure, temperature, and material. The variation in total tank mass is only caused by the geometry parameters. It is interesting to note that when all other parameters are equal, minimizing R will minimize tank mass. This is generally true because, in Eq. (12), R is proportional to t_{wall}.

4 Conclusion

This article describes the methodology of pressure vessel estimation and explains the analysis logic behind the estimations. The methodology is intended to assist in the conceptual design of pressure vessels and to evaluate the potential performance of pressure tanks in both mobile and stationary applications for the storage of hydrogen for fuel cell applications. With its range of tank types and materials, it can be used not only to size gaseous hydrogen storage systems but for systems using hydrogen storage materials as well. The temperature and pressure ranges allow tank mass, volume, and cost estimates for cryo-adsorbents down to 80 K and metal hydrides up to 250 °C.

This methodology estimates the size, shape, mass, and material cost of a hydrogen pressure vessel. The tool does not replace the formal pressure vessel design process, but its output can be considered the starting point for an actual pressure vessel design. Estimates provided by this methodology have matched real pressure vessel design characteristics within ±10%, making it a useful estimation tool.

Nomenclature

F = safety factor
K_{fte} = fiber translation efficiency factor
L = tank internal length
M = mass of tank
P = internal pressure
R = tank internal radius
Sd = design strength
Su = ultimate strength
Sy = yield strength
t_{wall} = wall thickness
V = tank internal volume
ρ = mass density
σ_{eqv} = Von Mises stress
σ_1 = principal stress 1
σ_2 = principal stress 2
σ_3 = principal stress 3

References

[1] Hydrogen Materials Advanced Research Consortium (HyMARC), 2023, "Hydrogen Storage Systems Modeling," U.S. Department of Energy, Office of Energy Efficiency & Renewable Energy, Washington, DC, accessed Nov. 17, 2023, https://www.hymarc.org/models.html
[2] Satyapal, S., Petrovic, J., Read, C., Thomas, G., and Ordaz, G., 2007, "The U.S. Department of Energy's National Hydrogen Storage Project: Progress Towards Meeting Hydrogen-Powered Vehicle Requirements," Catal. Today, **120**(3–4), pp. 246–256.
[3] Murray, L. J., Dincă, M., and Long, J. R., 2009, "Hydrogen Storage in Metal-Organic Frameworks," Chem. Soc. Rev., **38**(5), p. 1294.
[4] Ahluwalia, R. K., Hua, T. Q., Peng, J.-K., Lasher, S., McKenney, K., and Sinha, J., "Technical Assessment of Cryo-Compressed Hydrogen Storage Tank Systems for Automotive Applications," Argonne National Laboratory, Argonne, IL, Report No. ANL/09-33.
[5] Eaves, S., and Eaves, J., 2004, "A Cost Comparison of Fuel-Cell and Battery Electric Vehicles," J. Power Sources, **130**(1–2), pp. 208–212.
[6] Unterlohner, F., 2021, "Comparison of Hydrogen and Battery Electric Trucks," Transport & Environment, Brussels, Belgium, accessed Nov. 17, 2023, www.transportenvironment.org/wp-content/uploads/2021/07/2020_06_TE_comparison_hydrogen_battery_electric_trucks_methodology.pdf
[7] U.S. Department of Energy, 2023, "Fuel Cell Vehicles, - Benefits and Challenges," U.S. Department of Energy, Office of Energy Efficiency & Renewable Energy, Washington, DC, accessed Nov. 17, 2023, www.fueleconomy.gov/feg/fcv_benefits.shtml
[8] Cox, B., Bauer, C., Beltran, A. M., van Vuuren, D. P., and Mutel, C. L., 2020, "Life Cycle Environmental and Cost Comparison of Current and Future Passenger Cars Under Different Energy Scenarios," Appl. Energy, **269**, p. 115021.
[9] Hydrogen and Fuel Cell Technologies Office, 2021, "DOE Technical Targets for Onboard Hydrogen Storage for Light-Duty Vehicles," U.S. Department of Energy, Office of Energy Efficiency & Renewable Energy, Washington, DC, accessed Dec. 16, www.energy.gov/eere/fuelcells/doe-technical-targets-onboard-hydrogen-storage-light-duty-vehicles
[10] García-Holley, P., Schweitzer, B., Islamoglu, T., Liu, Y., Lin, L., Rodriguez, S., Weston, M. H., Hupp, J. T., Gómez-Gualdrón, D. A., Yildirim, T., and Farha, O. K., 2018, "Benchmark Study of Hydrogen Storage in Metal-Organic Frameworks Under Temperature and Pressure Swing Conditions," ACS Energy Lett., **3**(3), pp. 748–754.
[11] Ahmed, A., Seth, S., Purewal, J., Wong-Foy, A. G., Veenstra, M., Matzger, A. J., and Siegel, D. J., 2019, "Exceptional Hydrogen Storage Achieved by Screening Nearly Half a Million Metal-Organic Frameworks," Nat. Commun., **10**(1), p. 1568.
[12] Andersson, J., and Grönkvist, S., 2019, "Large-Scale Storage of Hydrogen," Int. J. Hydrogen Energy, **44**(23), pp. 11901–11919.
[13] Markert, F., Melideo, D., and Baraldi, D., 2013, "Uncertainties in Risk Assessment of Hydrogen Discharges From Pressurized Storage Vessels at Low Temperatures," Fifth International Conference on Hydrogen Safety, ICHS, Brussels, Belgium, Sept. 9–11.
[14] Brooks, K. P., Sprik, S. J., Tamburello, D. A., and Thornton, M. J., 2020, "Design Tool for Estimating Metal Hydride Storage System Characteristics for Light-Duty Hydrogen Fuel Cell Vehicles," Int. J. Hydrogen Energy, **45**(46), pp. 24917–24927.

[15] Grady, C., McWhorter, S., Sulic, M., Sprik, S. J., Thornton, M. J., Brooks, K. P., and Tamburello, D. A., 2022, "Design Tool for Estimating Adsorbent Hydrogen Storage System Characteristics for Light-Duty Fuel Cell Vehicles," Int. J. Hydrogen Energy., **47**(69), pp. 29847–29857.

[16] Niaz, S., Manzoor, T., and Pandith, A. H., 2015, "Hydrogen Storage: Materials, Methods and Perspectives," Renewable Sustainable Energy Rev., **50**, pp. 457–469.

[17] Holladay, J. D., Brooks, K. P., Rönnebro, E. C. E., Simmons, K. L., and Weimar, M. R., 2013, "Systems Engineering of Chemical Hydrogen, Pressure Vessel, and Balance of Plant for Onboard Hydrogen Storage," DOE Hydrogen and Fuel Cells Program, Washington, DC, FY2012 Annual Progress Report, Report No. PNNL-21567.

[18] Holladay, J. D., Brooks, K. P., Simmons, K. L., Rönnebro, E. C. E., and Weimar, M. R., "Systems Engineering of Chemical Hydrogen Storage, Pressure Vessel, and Balance of Plant for Onboard Hydrogen Storage," FY2013 Annual Progress Report, DOE Hydrogen and Fuel Cells Program.

[19] Barthélémy, H., Weber, M., and Barbier, F., 2017, "Hydrogen Storage: Recent Improvements and Industrial Perspectives," Int. J. Hydrogen Energy, **42**(11), pp. 7254–7262.

[20] Meyer, K., Pignagnoli, F., Potts, D., and Hunter, G., 2014, "Lightweighting Matters in Energy Storage," Reinforced Plastics, **58**(4), pp. 20–23.

[21] Moradi, R., and Groth, K. M., 2019, "Hydrogen Storage and Delivery: Review of the State of the Art Technologies and Risk and Reliability Analysis," Int. J. Hydrogen Energy, **44**(23), pp. 12254–12269.

[22] Darkrim, F. L., Malbrunot, P., and Tartaglia, G. P., 2002, "Review of Hydrogen Storage by Adsorption in Carbon Nanotubes," Int. J. Hydrogen Energy, **27**(2), pp. 193–202.

[23] Motyka, T., 2014, *Hydrogen Storage Engineering Center of Excellence Metal Hydride Final Report*, Savannah River National Laboratory, Aiken, SC.

[24] Ahluwalia, R. R. K., Peng, J.-K., and Hua, T. Q., 2016, "5-Cryo-Compressed Hydrogen Storage," *Compendium of Hydrogen Energy*, Woodhead Publishing, Argonne National Laboratory, Argonne, IL.

[25] Corgnale, C., Hardy, B., Chahine, R., Zacharia, R., and Cossement, D., 2019, "Hydrogen Storage in a Two-Liter Adsorbent Prototype Tank for Fuel Cell Driven Vehicles," Appl. Energy, **250**, pp. 333–343.

[26] ANSYS, 2017, *ANSYS Mechanical User's Guide, Release 18.1*, ANSYS, Canonsburg, PA.

[27] Brooks, K. P., Alvine, K. J., Johnson, K. I., Klymyshyn, N. A., Pires, R. P., Rönnebro, E., Simmons, K. L., et al., 2016, "PNNL Development and Analysis of Material-Based Hydrogen Storage Systems for the Hydrogen Storage Engineering Center of Excellence," Pacific Northwest National Laboratory, Richland, WA, Report No. PNNL-25234.

[28] Hardy, B., Tamburello, D., and Corgnale, C., 2018, "Hydrogen Storage Adsorbent Systems Acceptability Envelope," Int. J. Hydrogen Energy, **43**(42), pp. 19528–19539.

[29] Jaramillo, D. E., Jiang, H. Z. H., Evans, H. A., Chakraborty, R., Furukawa, H., Brown, C. M., Head-Gordon, M., and Long, J. R., 2021, "Ambient-Temperature Hydrogen Storage Via Vanadium(II)-Dihydrogen Complexation in a Metal–Organic Framework," J. Am. Chem. Soc., **143**(16), pp. 6248–6256.

[30] Klymyshyn, N. A., 2013, "PNNL Tank Mass Estimator for Cross Comparison of Type 1, Type 3, and Type 4 Pressure Vessels ("Tankinator")," Pacific Northwest National Laboratory, Richland, WA, Report No. Pnnl-SA-93460.

[31] Klymyshyn, N. A., and Barrett, N. P., 2022, "PNNL Tank Mass Estimator for Cross Comparison of Type 1, Type 3, and Type 4 Pressure Vessels ("Tankinator")," Pacific Northwest National Laboratory, Richland, WA, Report No. Pnnl-SA-179141.

[32] Sprik, S., Brooks, K., Grady, C., and Thornton, M., 2022, "Hydrogen Storage System Modeling: Public Access, Maintenance, and Enhancements," DOE Hydrogen Program 2022 Annual Merit Review and Peer Evaluation Meeting, Washington, DC, p. 23, accessed Mar. 2023, https://www.hydrogen.energy.gov/pdfs/review22/st008_thornton_2022_p.pdf

[33] Budynas, R., and Nissbett, J. K., 2006, "Shigley's Mechanical Engineering Design," McGraw-Hill Companies, New York.

[34] ASME, 2021, *ASME Boiler and Pressure Vessel Code*, American Society of Mechanical Engineers, New York.

[35] Oberg, E., Jones, F. D., Horton, H. L., and Ryffel, H. H., 2012, *Machinery's Handbook*, 29th ed., Industrial Press, Incorporated, New York.

[36] Hua, T. Q., Roh, H.-S., and Ahluwalia, R. K., 2017, "Performance Assessment of 700-Bar Compressed Hydrogen Storage for Light Duty Fuel Cell Vehicles," Int. J. Hydrogen Energy, **42**(40), pp. 25121–25129.

[37] Toray, 2018, "T700S Standard Modules Carbon Fiber," Toray Composite Materials America, Inc., Tacoma, WA, T700S Rev. 4: Updated April 13, 2018, accessed Dec. 16, 2021, https://www.toraycma.com/wp-content/uploads/T700S-Technical-Data-Sheet-1.pdf.pdf

[38] Holladay, J. D., Brooks, K. P., Simmons, K. L., Ronnebro, E., Weimar, M. R., Karkamkar, A. J., Devarakonda, M. N., et al., 2012, "Systems Engineering of Chemical Hydride, Pressure Vessel, and Balance of Plant for On-Board Hydrogen Storage," Presented by Jamie Holladay at DOE Fuel Cell Program Annual Merit Review, Washington, DC, Paper No. PNNL-SA-86976, accessed Jan. 28, 2022, https://www.hydrogen.energy.gov/pdfs/review12/st005_holladay_2012_o.pdf

[39] Tamburello, D., Hardy, B., Corgnale, C., Sulic, M., and Anton, D., 2017, "Cryo-Adsorbent Hydrogen Storage Systems for Fuel Cell Vehicles," ASME Paper No. FEDSM2017-69411.